

ITC 3/51 Information Technology and Control Vol. 51 / No. 3 / 2022 pp. 531-544 DOI 10.5755/j01.itc.51.3.29322	Texture Image Analysis for Larger Lattice Structure Using Orthogonal Polynomial Framework	
	Received 2021/06/23	Accepted after revision 2022/02/27
	 <a href="http://dx.doi.org/10.5755/j01.itc.51.3.29322">http://dx.doi.org/10.5755/j01.itc.51.3.29322</a>	

**HOW TO CITE:** Ganesan, L., UmaRani, C. Kaliappan, M., Vimal, S., Kadry, S. Nam, Y. (2022). Texture Image Analysis for Larger Lattice Structure Using Orthogonal Polynomial Framework. *Information Technology and Control*, 51(3), 531-544. <http://dx.doi.org/10.5755/j01.itc.51.3.29322>

# Texture Image Analysis for Larger Lattice Structure Using Orthogonal Polynomial Framework

## L. Ganesan

Ramco Institute of Technology, Rajapalayam, Tamil Nadu, India; e-mail: [principal@ritrjpm.ac.in](mailto:principal@ritrjpm.ac.in)

## C. UmaRani

A C Govt. College of Engineering and Technology, Karaikudi, India; e-mail: [drcumakkd@gmail.com](mailto:drcumakkd@gmail.com)

## M. Kaliappan

Ramco Institute of Technology, Rajapalayam, Tamil Nadu, India; e-mail: [kaliappan@ritrjpm.ac.in](mailto:kaliappan@ritrjpm.ac.in)

## S. Vimal

Ramco Institute of Technology, Rajapalayam, Tamil Nadu, India; e-mail: [vimal@ritrjpm.ac.in](mailto:vimal@ritrjpm.ac.in)

## Seifedine Kadry

Department of Applied Data Science, Noroff Universty College, Kristiansand, Norway

Department of Electrical and Computer Engineering, Lebanese American University, Byblos, Lebanon

## Yunyoung Nam

Soonchunhyang University, Asan; Republic of Korea; e-mail: [ynam@sch.ac.kr](mailto:ynam@sch.ac.kr)

---

Corresponding author: [ynam@sch.ac.kr](mailto:ynam@sch.ac.kr)

---

An Orthogonal Polynomial Framework using 5 x5 mathematical model is proposed and attempted for the texture image analysis. The Orthogonal Polynomial Framework has been shown effective for image with larger image grid size of (5 x 5) or (7 x 7) or (9\*9) or even higher, to analyse textured surfaces. The image region (5 x 5) under consideration is evaluated to be textured or untextured using a statistical approach. The textured region is represented locally as well as globally by suitable descriptors for further analysis. The local descriptor is termed as pro5num and histogram of these pro5nums is called the pro5spectrum, the global descriptor. The novelty of this scheme is its representation of texture after it identifies the presence and the model can be extended to any image size region. This method works fine for standard database of texture images. The texture images have been shown successfully represented by the descriptors. The proposed scheme has been successfully applied for the supervised texture classification and the classification accuracies are comparable with recent results. Further texture analysis problems using these descriptors are in progress.

**KEYWORDS:** Texture Representation, Polynomials, Statistical Tests, Local and Global descriptors, Standard Texture Images, Classification.

---

## 1. Introduction

An image is considered to be consisting of either textured or un-textured or uniform distribution of gray levels. The presence of uniform region can be easily identified by the constant grey levels maintained by the pixels throughout. The presence of edges are found by detecting the sharp grey level variations among the pixels or between the regions whereas the texture is presumed to be present if there is a non-uniform grey level variations in the small region. There have been many algorithms proposed separately over the past [4, 9, 10, 13], for identifying the presence of texture. The texture can be classified as micro, macro, deterministic, non-deterministic, periodic, aperiodic, regular, irregular, smooth, rough, fine, coarse, and stochastic based on the distribution of textural properties. Since the underlying textural content of images appear to convey many distinguishing quantitative features for classification purposes. In this paper, we propose a suitable framework which is used for finding the presence of texture in (5x5) region.

For analysis of texture, various schemes have been reported in literature. Observable textures [5] were suggested which are analysed by the primitives and their placement rules. Haralick et al [10] have suggested using the co-occurrence matrix and proposed variety of features. Tuceryan, and Weszka [13,14], suggested the Fourier Power spectrum and descriptor based texture analysis. Texture number scheme has been suggested by He and L Wang [11] and multi-channel filtering approach by Jain et al [12]. Ganesan and Bhattacharrya [7] have suggested micro texture description based on

design of experiments approach. Local description of texture has been a quite challenging problem still.

Spatial filtering approach has been employed for texture analysis by [10]. Relatively a larger image region, say (5x5) is considered for our present analysis since already the analysis for 3x3 image region has been reported which was noise sensitive. In a (3 x 3) image region, even the presence of noise may cause the variation in the texture. To avoid this problem, an image region of size, (5x5), which is relatively larger, is chosen in our present work so as to reduce the effect of noise, as it may get blurred over a larger region. The influence of noise will be less and not disturbing the presence of signal, namely, texture in the present work. The image region is represented by a set of orthogonal polynomials, the corresponding orthogonal effects owing to the spatial variations and their variances can be computed. The design of experiments based approach suggests that there are two kinds of variances, namely, the variances due to the main effects and the other one is the variances due to the interaction effects. In a two dimensional case, the main effects are from the variations of x coordinate when the y remains constant whereas, the interaction effects are due to the variations of both x and y coordinates jointly. It has been found experimentally that the interaction effects convey the presence of micro textures and the main effects, on the other hand, the noise. The presence of textures can be confirmed when the interaction effect variances are significant while the variances due to the main effects are con-

tributing toward noise, i.e., they are estimates of same variances and homogeneous. These variances are tested for the homogeneity, by performing a statistical test proposed by Bishop and Nair [1] since the mean squares due to these effects are varying in Chi squared form with single degree of freedom. The test can be performed for a specific tolerance value, say 1% or 5% and so on. If the test is performed for 1%, it is denoted that the conditions are stringent and if it is 5% it is in relaxed. After this test, the average error variance is computed from the set of variances or its subset, which are estimates of the same variance. Similarly, the variances of interaction effects must be tested for the heterogeneity. The test can be performed with all the variances of interaction effects or its subsets. Once homogeneity of variances test is over and the region is concluded to be textured. Then the region has to be represented. All the variances corresponding to the interaction effects or its subsets are subjected to the variance ratio statistical test [6]. Numerator as the variance of the interaction effects and the denominator is the average error variance. When the ratio is greater than or equal to the standard tabulated value, (known as F ratio test) then the corresponding pixel position is marked as 1 otherwise 0. The variance ratio test can also be performed by different significance levels. Thus there is a mapping of interaction effects in to 0 or 1. If these binary numbers are written as a sequence, i.e., a binary string is obtained corresponding to the set of variances used for the significant interaction effects. The equivalent decimal number for this binary string is termed as the  $pro5num$ . This quantifiable value is used for representing the texture present in the (5x5) region. Hence a (5x5) region is represented by  $pro5num$  which is called the local descriptor. Since the grey level distributions over the entire image is unique which contribute for the information, the  $pro5nums$  and their distribution is also unique. The entire image now is represented globally by the distribution of these  $pro5nums$ , called,  $pro5spectrum$ . The  $pro5spectrum$ s are the unique representation of the given image.  $Pro5spectrum$ s are obtained for a number of standard texture images, called Brodatz album [2]. The variations in the  $spectrum$ s and the number of  $pro5nums$  present in the  $spectrum$ s differ for different images as expected. The usages of these  $pro5spectrum$ s are subjected to various kinds of texture analysis problems. The Bayesian framework and PAC assembling

suggests the usage of DL for image classification, another approach to handle the Large Lattice structure [15], [16]. The full stage augmentation data has been utilised for the image classification in many lattice structure where the Deep learning algorithms like CNN, RNN and LSTM proposes a valid framework [17],[18]. Texture classification of fabric defects has been successfully attempted using machine learning techniques [19].

The complete framework and the mathematical model is discussed in the next section. The experimentation works and results are described in the III section and finally in the IV section, the conclusions are presented.

## 2. Mathematical Model

A 2D image is considered around  $x$  and  $y$  which are Cartesian coordinates, separable, blurring, point spread operator (PSF) in which the image results in the superposition of the point source of impulse weighted by the value of object function  $f$ . A 2D PSF,  $M(x,y)$  can be considered to be a real valued function defined for  $X \times Y$  where  $X$  and  $Y$  are ordered subsets of real values. In the case of a gray level image of size  $(n \times n)$  where  $x$  rows consists of a finite set, which is as  $0,1,2,\dots,n-1$ , the function  $M(x,y)$  reduces labeled to a sequence of function.

$$M(i, t) = \gamma_i(t), i = 0,1,2,\dots,n-1.$$

The mathematical model used in this framework is illustrated below.

Since the image is a function of  $f(x, y)$  where  $x$  and  $y$  are Cartesian coordinates, a set of polynomials for fitting with image region is used. The image region,  $f(x, y)$  is represented as

$$f(x, y) = g(x, y) + \eta(x, y),$$

where  $g(x, y)$  is the signal part and  $\eta(x, y)$  is the additive noise. The characteristics of the image region, like texture/uniform, or edge, etc. can be identified by analyzing the spatial variation in  $g(x, y)$ . These characteristics can be obtained by using the spatial (row and column) interactions. These spatial interactions are measured here by fitting the image region with a set of polynomials, in row and column coordinates. A set of orthogonal polynomials are preferred by as

it reduces the time complexity while processing. Let us consider a set of orthogonal functions  $\alpha_{i,j}(x,y)$  which are used to obtain the spatial interactions due to signal and noise. Hence

$$f(x,y) = \sum_i \sum_j \beta_{i,j} \alpha_{i,j}(x,y) + \eta(x,y) \tag{1}$$

original image region = spatial variation due to signal + spatial variation due to noise.

In general,

$$f(x,y) = \sum_i \sum_j \beta_{i,j} \phi_i(x) \phi_j(y) \text{ as } \alpha_{i,j}(x,y) \text{ separable} \tag{2}$$

Let  $\beta_{i,j}$  be the orthogonal effects which are the coefficients of transformations for fitting the polynomials with the image region.

$$f(x,y) = \sum_i \sum_j \beta_{i,j} \gamma_i \gamma_j \tag{3}$$

where  $\gamma_i$  and  $\gamma_j$  are the polynomials in x and y respectively. In matrix notation, this can be written as,

$$[f] = \sum \sum \beta_{i,j} \gamma_i \hat{\gamma}_j^t \tag{4}$$

where  $\hat{\gamma}_i$  is a column vector of size (N x 1).

Considering the values of the polynomials

$$\gamma_i(r) \text{ at } r = r_1, r = r^2 \dots r = r_n$$

Now

$$[M] = \begin{bmatrix} \hat{\gamma}_0 \\ \hat{\gamma}_1 \\ \hat{\gamma}_2 \\ \dots \\ \hat{\gamma}_{n-1} \end{bmatrix}$$

$$[f] = [M][\beta_{i,j}] [M]^t$$

By algebraic simplification

$$[\beta_{i,j}] = (M^t M)^{-1} (M^t f M) (M^t M)^{-1} \tag{5}$$

In the following section, the generation of polynomials and how this is generalized to get n<sup>th</sup> order polynomials are discussed. Once the generation is over, representation will be described.

### 2.1. Polynomials

For computation of spatial interactions, the following polynomials are used.  $\gamma_0(r, \mu, n)$ ,  $\gamma_1(r, \mu, n)$  of degree 0, 1, ..., where  $\mu$  represents mean

$$\mu = \frac{1}{n} \sum_{r=1}^n r = \frac{n+1}{2}$$

where n is the image sample size, n = 5.

$$\gamma_0(r, \mu, n) = 1, \gamma_1(r, \mu, n) = r - \mu$$

Higher order polynomials can be generated by employing (Generalised Chebhevsev Formula)

$$\gamma_{i+1}(r, \mu, n) = (r - \mu) \gamma_i(r, \mu, n) - s_i(r) \gamma_{i-1}(r, \mu, n) \text{ for } i \geq 1. \tag{6}$$

$$s_i(n) = \frac{i^2(n+i)(n-i)}{4(4i^2-1)}. \tag{7}$$

Finally, the following set of orthogonal polynomials are obtained. Where  $s_i$  is represented as the polynomial generating factor, with two variables, i and n, used to compute  $\gamma_0, \gamma_1, \gamma_2, \gamma_3, \gamma_4$  and can be shown in Equation (8).

$$\gamma_0(r, \mu, n) = 1$$

$$\gamma_1(r, \mu, n) = r - \mu \text{ where } \mu = \frac{n+1}{2}$$

$$\gamma_2(r, \mu, n) = (r - \mu)^2 - \frac{(n^2 - 1)}{12}$$

$$\gamma_3(r, \mu, n) = (r - \mu)^3 - \frac{(r - \mu)(3n^2 - 7)}{20} \tag{8}$$

$$\gamma_4(r, \mu, n) = (r - \mu)^3 - \frac{(r - \mu)^2(r - \mu)(3n^2 - 13)}{14} + \frac{3n^4 - 30n^2 + 27}{560}$$

Typically, for example,

$$\text{when } r_0 = 1, r_1 = 2, r_2 = 3, r_3 = 4, r_4 = 5$$

$$\gamma_1(r_0) = 1 - 3 = -2,$$

$$\gamma_1(r_1) = 2 - 3 = -1,$$

$$\gamma_1(r_2) = 3 - 3 = 0,$$

$$\gamma_1(r_3) = 3 - 4 = -1,$$

$$\gamma_1(r_4) = 3 - 5 = -2$$

Similarly, other  $\gamma_i$  such as  $\gamma_2, \gamma_3, \gamma_4$  can be obtained.

Thus for an (n x n) i.e. (5 x 5) image region.

$$|M| = \begin{bmatrix} \gamma_0(r_0) & \gamma_1(r_0) & \gamma_2(r_0) & \gamma_3(r_0) & \gamma_4(r_0) \\ \gamma_0(r_1) & \gamma_1(r_1) & \gamma_2(r_1) & \gamma_3(r_1) & \gamma_4(r_1) \\ \gamma_0(r_2) & \gamma_1(r_2) & \gamma_2(r_2) & \gamma_3(r_2) & \gamma_4(r_2) \\ \gamma_0(r_3) & \gamma_1(r_3) & \gamma_2(r_3) & \gamma_3(r_3) & \gamma_4(r_3) \\ \gamma_0(r_4) & \gamma_1(r_4) & \gamma_2(r_4) & \gamma_3(r_4) & \gamma_4(r_4) \end{bmatrix} \tag{9}$$

$$|M| = \begin{bmatrix} 1 & -2 & 2 & -1 & 1 \\ 1 & -1 & -1 & 2 & -4 \\ 1 & 0 & -2 & 0 & 6 \\ 1 & 1 & -1 & -2 & -4 \\ 1 & 2 & 2 & 1 & 1 \end{bmatrix}$$

The gray level image region of size (5 x 5),

$$[f_{i,j}^5] = |M||\beta| = \sum_{i=0}^4 \sum_{j=0}^4 \beta_{i,j} |C_{i,j}|. \tag{10}$$

$\beta_{i,j}$  is representing the variation effect due to  $|C_{i,j}|$  on  $f$  and the effects  $\beta_{i,j}$  are orthogonal to each other. 25 basis 2D operators  $C_{i,j}$  ( $0 \leq i, j \leq 4$ ) can be obtained as follows:

$$C_{i,j} = \hat{\gamma}_i \otimes \hat{\gamma}_j^t,$$

where  $\hat{\gamma}_i$  is the  $(i + 1)$ st column vector of  $|M|$ . Now the image region  $f$  is viewed as superposition – of 25 basis finite difference operators’ responses, of which  $|C_{0,0}|$  is meant for local averaging. These basis operators can be generated. Hence

$$|f| |f| = |Z| |Z|$$

$$\sum_{i=0}^4 \sum_{j=0}^4 Image_{i,j}^2 = \sum_{i=0}^4 \sum_{j=0}^4 Variances_{i,j}^2 \tag{11}$$

$Z_{i,j}^2$  may be termed as the variances corresponding to the  $(n^2 - 1)$  basis difference operators. As per the intuitive guidelines given by Canny [3], we model the texture as the responses of the operators

$$|C_{i,j}|, i, j = 1 \text{ to } 4$$

and the responses of the remaining operators, namely,

$$|C_{i,j}|, i = 0 \text{ and } j = 1, 2, 3, 4 \text{ and } j = 0 \text{ and } i = 1, 2, 3, 4$$

to be the responses towards noise present.

$$[\beta_{i,j}] = (M^t M)^{-1} (\beta'_{i,j}) (M^t M)^{-1}, \tag{12}$$

where  $M$  is in Equation (9).

From Equation (5),

$$[\beta'_{i,j}] = (M^t f M) \text{ and } [f] \text{ is an image region of size } (5 \times 5).$$

The mean square variances due to these orthogonal effects can be computed as

$$[Z_{i,j}^2] = ([M^t][M])^{-1} (\beta'_{i,j})^2 ([M^t][M])^{-1}, \tag{13}$$

where  $Z_{i,j}^2$  are the variances of each pixel when the image regions are mapped.

For texture, the conjecture [7] says that the mean squares or variances due to interaction effects do not estimate the same variance (heterogeneous) and the mean squares due to main effects may estimate the same variance (homogeneous). Statistical test : This homogeneity of variations test can be performed by a statistical procedure called Nair’ test [1]. Nair’s Test:

The divergence  $D$  among variances,  $v_i, i = 1, 2, \dots, k$  is computed as follows:

$$D = k \ln(v_{av}) - \sum_{i=1}^k \ln(v_i) \tag{14}$$

$$v_{av} = \frac{1}{k} \sum_{i=1}^k \ln(v_i). \tag{15}$$

Standard values are given (tabulated) as Bishop and Nair’s table for different values of degrees of freedom and different percentage of significance levels and are shown in (Table 1). The interaction means squares are subjected to Nair’s test. The  $D$  value must be  $\geq$  to the tabulated value indicating that the divergence is significant. If it is  $\leq$  the values given in the table, indicating the divergence is insignificant and hence these can be considered for computing noise variances. Once the conditions are satisfied, then the image region under analysis is considered as textured region. This region is to be represented as per the procedure in the following section.

**Table 1**  
Divergence Values

Tolerance	Degrees of Freedom (DoF)					
	2	3	4	5	6	7
5%	5.1	7.7	10.0	12.0	14.1	15.9
1%	8.3	11.5	14.0	16.5	18.9	21.0
Degrees of Freedom						
	8	9	10	15	20	
5%	17.9	19.6	21.3	29.9	37.9	
1%	23.1	25.2	27.2	36.5	45.3	

**2.2. Representation**

Detected textured regions must be represented locally and the entire image globally by suitable descriptors.

- 1 Local: Mean Square error variance (msv) is computed from the main effect mean squares, namely,  $m_1$  to  $m_8$  as in Equation (16) or its subsets, which are estimates of same variance divided by the total degrees of freedom.
- 2 Mean Square variance, due to contributing interaction effects, must be significant compared to the msv.

**Table 2**  
F Distribution Values

DoF	5%	10%	20%	25%	50%
2	18.51	8.53	3.56	2.59	0.667
3	10.13	5.54	2.68	2.02	0.585
4	7.71	4.54	2.35	1.80	0.548

This is checked by performing the variance ratio test as the  $Z_{ij}^2$ , which are belonging to the interaction effects which are distributed as the F distribution [6] with 1 and m degree of freedom where m is the number of  $Z_{ij}^2$  used to compute the error variance..

Set of standard values used in F statistical distribution are given in Table 2. F Test: Numerator/Denominator = one of the Mean squares due to the interaction effects / Mean square error variance. If this ratio  $\geq$  F tabulated value, then it is significant.

- 3 Significant interaction effects are represented by 1 else by 0.
- 4 Hence a mapping from image region to a sequence of binary members are obtained as follows. The equivalent decimal number for these binary numbers mentioned from a1 to a16 will be the texture representation, called local descriptor i.e., pro5num

$$\begin{bmatrix} p1 & p2 & p3 & p4 & p5 \\ p6 & p7 & p8 & p9 & p10 \\ p11 & p12 & p13 & p14 & p15 \\ p16 & p17 & p18 & p19 & p20 \\ p21 & p22 & p23 & p24 & p25 \end{bmatrix} = \begin{bmatrix} * & m1 & m2 & m3 & m4 \\ m5 & a1 & a2 & a3 & a4 \\ m6 & a5 & a6 & a7 & a8 \\ m7 & a9 & a10 & a11 & a12 \\ m8 & a13 & a14 & a15 & a16 \end{bmatrix} \quad (16)$$

Here  $p_i$  is the  $i^{th}$  pixel in the image region under consideration,  $m_1$  to  $m_8$  are the variances due to the main effects and  $a_1$  to  $a_{16}$  are the variances due to the interaction effects. If all 16 interaction effects are considered for the descriptor, it ranges from 0 to  $2^{16}$  which is relatively larger number. The number of significant interaction effects and their corresponding variances are to be found out. I.e, the subset of these variances are used for our experimentation to describe the local description. The texture primitives, manually generated with intensity values and collected from the test images are subjected to this test. These primitives are tested by including all the sixteen interaction effects and then lesser number of effects, considered at a time. There were so many combinations of interaction effects.

The number of samples pass the test are taken in to consideration. Over 600 such samples are subjected to texture detection experiments. The following four groups of interaction effects pass the test , i.e., pass in more than 80%. After the experiments, it was concluded that the interaction effects which are grouped as follows, which gave good results. Hence, from the total 16 interaction effects, a1 to a16 as in Equation (16),

*Group 1:  $a_2, a_5, a_7, a_{10}, a_{12}, a_{15}$ : Off the main diagonal elements.*

*Group 2:  $a_2, a_3, a_4, a_7, a_8, a_{12}$ : Upper triangular elements*

*Group 3:  $a_5, a_9, a_{10}, a_{13}, a_{14}, a_{15}$ : Lower triangular elements and*

*Group 4:  $a_1, a_2, a_5, a_6, a_7, a_{10}, a_{11}, a_{12}, a_{15}, a_{16}$ : Main diagonal and just off the diagonal elements*

are considered in our work.

These variances are subjected to Bishop and Nair test [1] for detecting the presence of texture, as given in the Equations (14)-(15). If the variances pass the test then it implies that there is a presence of texture. This region has to be represented which quantifies the content of texture in the prescribed tolerance levels. Once the region under consideration is found to be textured, this is represented by equivalent decimal number, called pro5num. Whatever may be the groups, the corresponding variances due to the interaction effects are termed as  $z_1, z_2, z_3$  and so on up to zn. With the interaction effects the local descriptor, pro5num is computed as follows.

$$\text{pro5num} = \sum_{i=1}^n z_i 2^{(i-1)}. \quad (17)$$

The value of pro5nums ranges from 0 to 63 (as there are six interaction effects in the first three groups). This is viewed as the binary string of six digits, varying from  $\{000000\}$  to  $\{111111\}$ . The corresponding decimal numbers varying from 0 to 63 as per Equation (17). If the fourth group is used, the number varies from 0 to 1023. It is just sufficient to use any one of the groups throughout the work. It would have been better if all the 16 interaction effects are considered for the representation. If all the 16 interaction effects are included for the computation of pro5nums, then the pro5num range will be from 0 to 65535 which is equivalent to the total number of pixels in case if the image size is 256 x 256. Generally, the representation must be simpler and describes the whole image. Thus, the above stated four groups are considered in our work.

### 3. Experimentation

#### 3.1. Global Representation

The proposal discussed in the previous section have been experimented with a large number of texture primitives. These divergence of variances test have been conducted and the number of samples passing the tests are computed for 1% and 5% significance or tolerance levels. The texture primitives collected from the texture images from a large database [2] are considered for our analysis. The four images D38, D84, D92, and D94 from Brodatz and six images from large VisTex databases [20] are shown in Figure 1.

At stringent conditions, i.e., 1% tolerance level, the four group of interactions are included for the experimentation. Various texture images such as D38, D82, D92, D94 selected from the standard Brodatz album [2] and six images from Vis Tex album [20] are used for the experimentation. For a given image, the pro5num, is computed using one of the four groups as stated in the previous section, considering 5 x 5 region at a time. This will be corresponding to the center pixel's position. The experiment is repeated by leaving one column, by including next column, another 5 x 5 region is considered. The corresponding pro5num will be the descriptor for this region and so on until the last pixels are completed. The frequency of occurrences of the pro5nums will be used for representing the entire image, called pro5spectrum. These are shown in Figure 2 for the image D38, represented in a bar chart. The remaining images have also been experimented and the same trend is maintained. Figure 2(a) shows only very few components present in the spectrum, indicating the limited number of samples pass the test.  $D = 1\%$  and  $F = 5\%$  significance levels are used with Group 1 interactions. The range of values of the pro5nums in this case will be 0-63. In the x axis, the values of pro5nums and the y axis, the frequency of occurrences of each pro5nums for the entire image, are used for drawing the pro5spectrums. Fig 2 b- d shows the pro5spectrums for the same image at different significance levels in F ratio test, namely, 10%, 20% and 50%, respectively. As the significance levels are getting relaxed from 5% to 50 %, the number of components present in the spectrums will be higher and higher. Figure 2(e-h), again shows the same variation with respect to F ratio and  $D = 5\%$  significance levels. The spectrums have almost all the values of

Figure 1

Images collected from Brodatz (a-d) and Vis Tex (e-j) Textural album

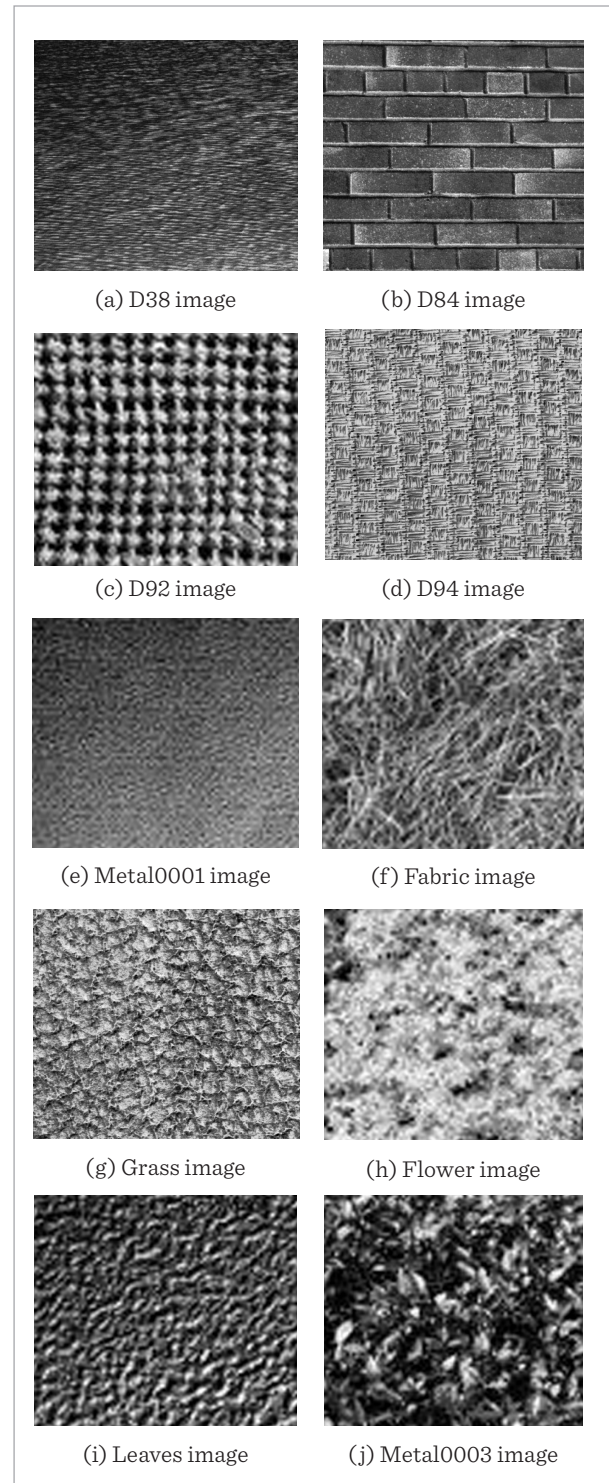
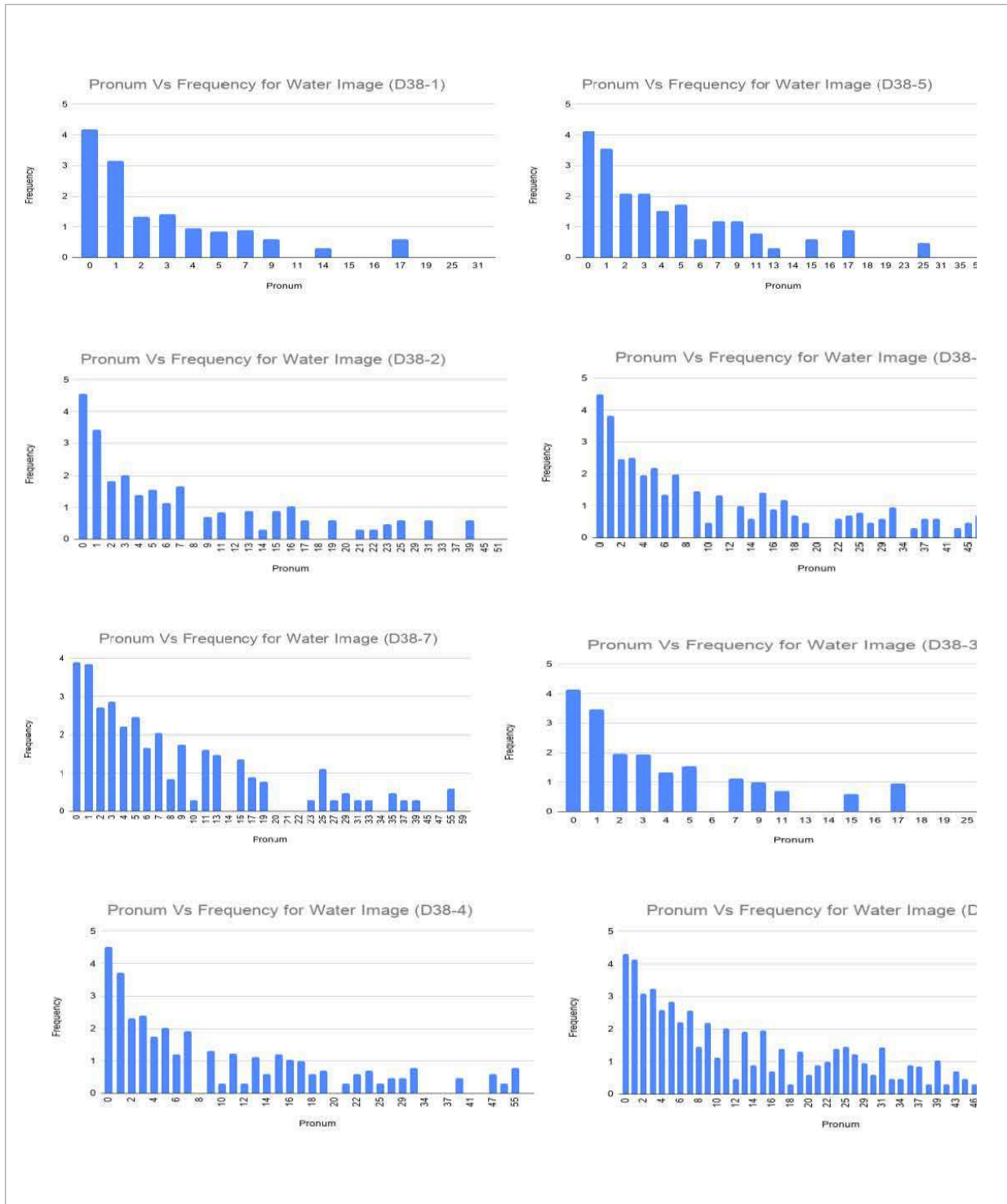


**Figure 2**

Pro5spectrums for the image D38 shown in Figure 1, [left column a-d, right column e-h, from top to bottom]



pro5nums because of the relaxation. If it is still relaxed, almost all the regions will have texture i.e., almost all the pixels will be replaced by the pro5nums yielding larger spikes for all the pro5nums. Figure 3 shows the pro5spectrums for D84 image using the group2 interactions. The previous conclusions hold good here also. The experiment is repeated for the group3 and group4 interactions. In group4 case, the pro5num ranges from 0 to 1023 indicating that the features are more. Using 5 x 5 image regions considered, very few literature have been presented. Hence the results have not been compared with any of the existing results. For the other images shown in Figure 1, namely, for example, D92 and D94, instead of showing the prospectrums as in Figure 2, the graphs are drawn, showing the number of components present in the pro5spectrums and the F ratio level (%) of relaxation. Number of components in the Y axis and the F ratio levels in the X axis, for the divergence lev-

el D at 1% and 5% respectively. These are shown in Figure 4, for four groups of interactions. As it is evident from the graphs in Figure 4 that as the levels are relaxed both in F and D, the number of components present in the graph are more. When Group 4 interactions are employed for obtaining the prospectrum, the pro5nums ranges vary from 0 to 1063, which is also visible from the graph in Figure 4. The experiment has been performed for the other images also shown in Figure 1. As it is evident that for D = 1%, the number of components present are less and will be higher in D = 5% cases.

The main claims in this work are as follows. For any given size of the image, the image regions are considered as (5 x 5) and is represented by mapping with a set of orthogonal polynomials. Based on the intensity values of the pixels present, the coefficients (orthogonal effects) for the polynomials will be different. Such orthogonal effects are carrying the relevant infor-

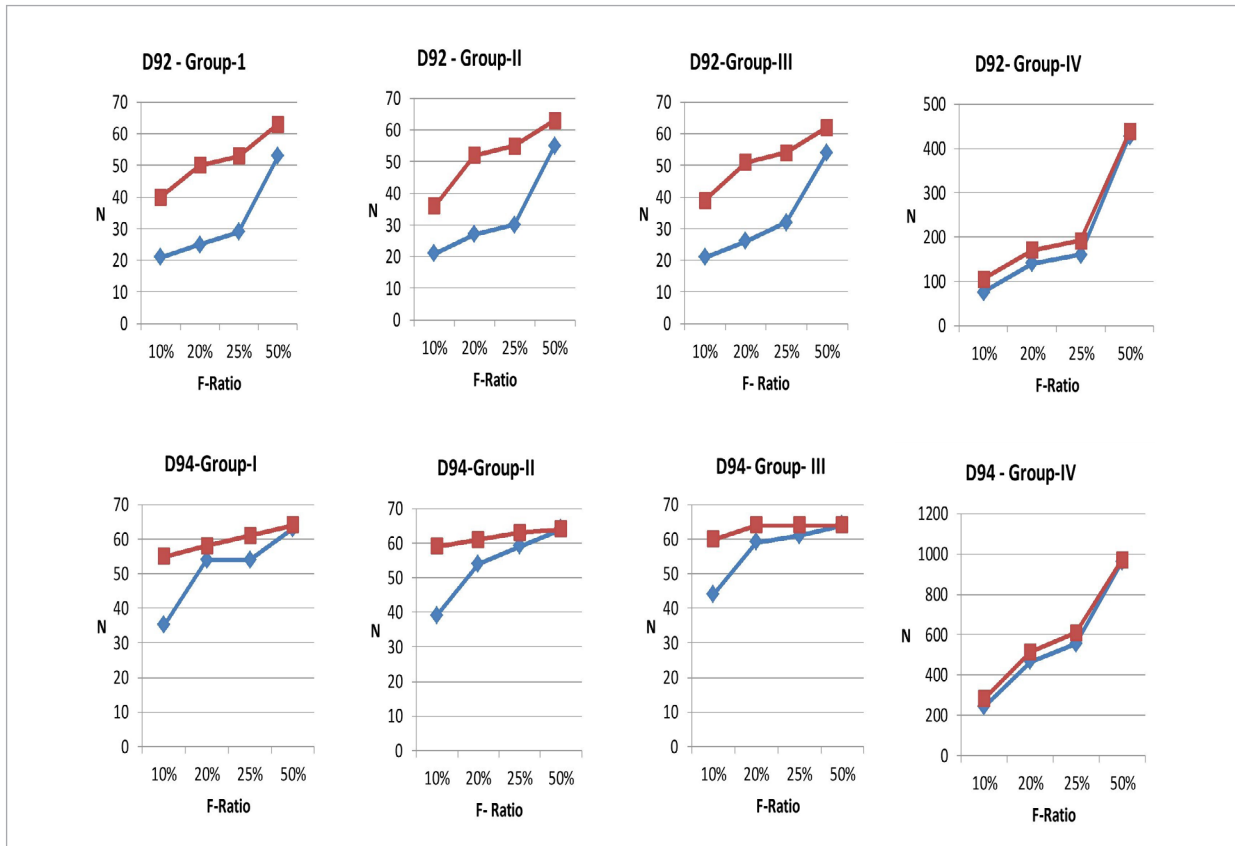
**Figure 3**

Pro5spectrums for the image D84 shown in Figure 1 [left column a-d, right column e-h, from top to bottom]



Figure 4

F ratio in % Vs Number of components in the spectrum (first row: for the image D92 – Grop I to IV Interactions, Red line indicates D= 5% and Blue for D = 1%). The second row for the image D94



mation. Using these effects and their corresponding variances, the experiments are performed: (i) Whether the region has the texture, presence can be identified, (ii) the texture content can be quantified using the local descriptor proposed; (iii) The frequency of occurrences of each  $pro5nums$  computed for the entire image is the global descriptor; (iv) One among the four groups of interaction effects may be chosen; (v) Since the gray levels variation for an image is unique, the  $pro5nums$  computed from such image regions and hence the  $pro5spectrums$  are also unique; (vi) For performing texture analysis experiments, instead of processing the entire images, the equivalent proposed descriptors may be used which is efficient in terms of both the complexities; (vii) This approach is developed from proven statistical principles and tests and (viii) the choice of groups and the tolerance levels can

be of users choice, (ix) processing still with a larger region, is possible if the polynomials are chosen accordingly (Polynomials of any order can be generated using the generalization formula give in Section 2).

Using these spectrums, the supervised and unsupervised classifications using the Deep Learning approach and segmentation with different edge detectors are under progress. The types of textures such as micro, macro, strong and weak, deterministic, etc. can be identified by the pattern of  $po5spectrums$ . This work is under progress. Variety of experiments have been conducted to establish the efficacy of the proposed framework.

The illumination and human perceiving concepts can be analogously said to match with different levels of tolerance levels. Since the micro texture appears almost in all the day to day surfaces, surfaces of metals,

composites, micro structures, abraded or fractured surfaces, etc. Hence the work is having more relevance to all types of applications, and the images can be analyzed at different significance levels. The microtexture contributes for all the variety of interactions, yielding to all the values present, having more components present in the spectrums. This uniqueness can be effectively used for representing the texture image globally. Thus, the local descriptor and global descriptors are working successfully. In order to compare our proposed work with the existing results, classification experiment is considered and explained in the following sub section.

### 3.2. Texture Classification

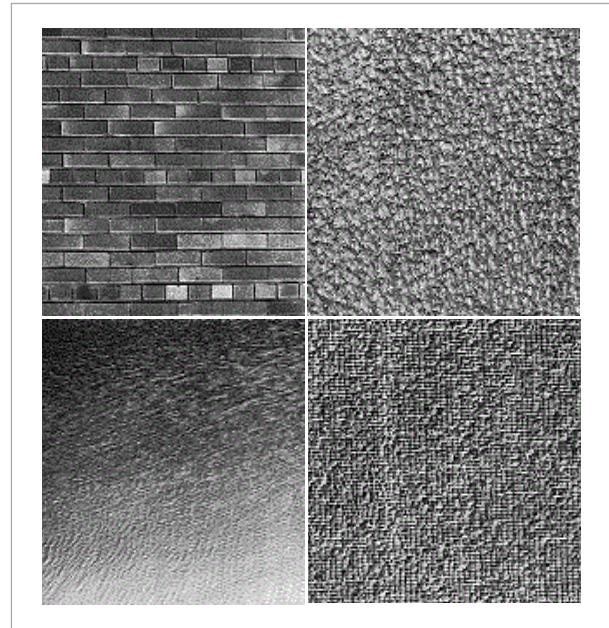
The proposed texture representation, namely, pro5spectrum, is now applied for performing in the supervised texture classification, for comparing the performance with recent results.

For any given texture image of size  $(m \times n)$ , the pro5spectrum can be obtained by following the procedure depicted in the previous section, for a particular D and F ratios which are similar to the ones shown in Figure 3. There are four texture images, namely, D94, D92, D38 and D84 [2] are considered for our experimentation. Portions of each image have been positioned in four quadrants of the target image (Figure 5). For performing the classification of the target image region to any one of the four classes in the reference spectrums which is the supervised classification. A window of size  $(15 \times 15)$  image regions are considered from each image (class) and their corresponding pro5spectrum are obtained called as reference spectrums.

A  $15 \times 15$  image region is considered from the target image, from the top left corner, and obtain the pro5spectrum. This spectrum will be compared with the values of the reference spectrums. The particular class will be assigned to the target region for which the distance between them is minimum. The distance measure used for finding the closeness is the integrated absolute difference between the spectrums. Once the target image region is identified to be closer to any one of the four classes, the centre position corresponding to the target region is marked as the particular class. Now the experiment is repeated by considering the adjacent region in the target image by including another column leaving the first column.

**Figure 5**

Target Image consists of D94, D92, D38 and D84 from [2]



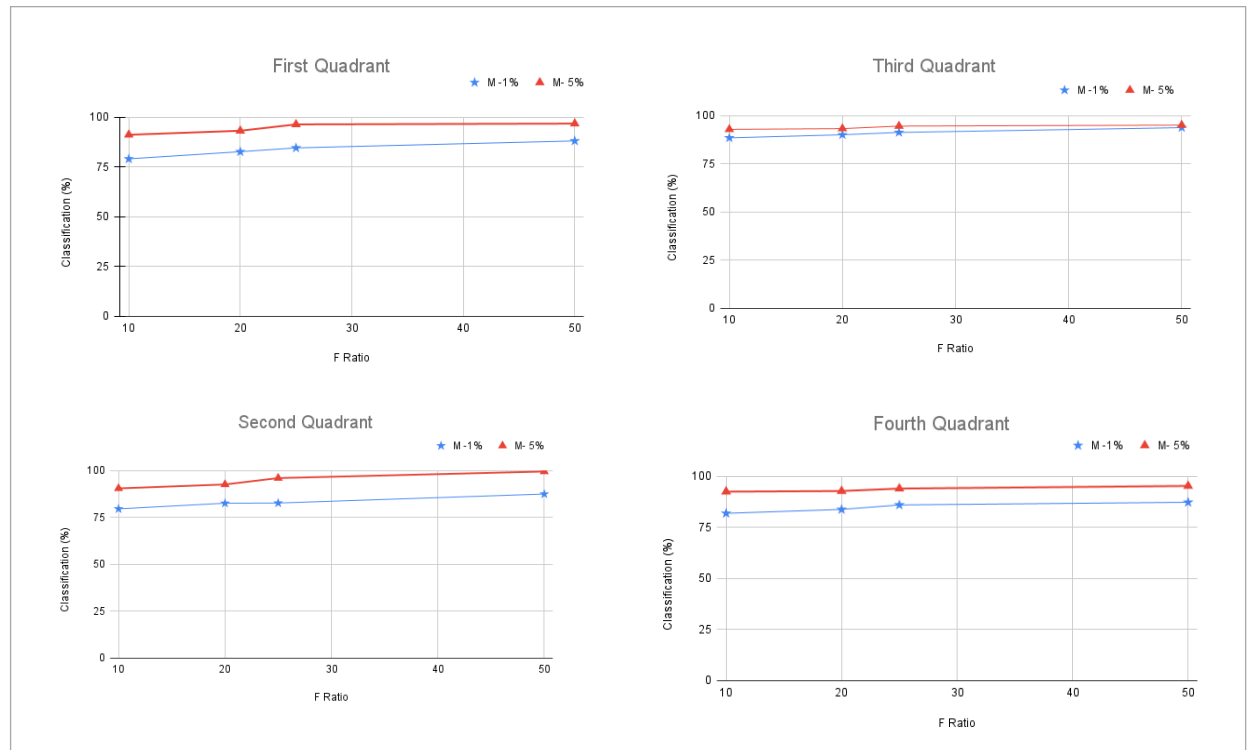
For this region, the class thus obtained is represented in the corresponding position of the result image. After completing the entire target image, the classes are represented based on the distance measure in the result image. The correct classification accuracy is obtained as the ratio of the number of pixels correctly classified to the total number of pixels in the target image, in each region. For first quadrant, count is obtained as the number of pixels correctly classified as 1, against the total number of pixels in the first quadrant. Some of the pixels may be wrongly classified to be 2 or 3 or 4, instead of 1. Such pixels correspond to the misclassified pixels. The experiment is repeated for different values of M and F ratios and the classification accuracy is obtained. The values are obtained and are tabulated as in Table 3. The corresponding graphs are drawn and shown in Figure 6.

It is evident that as the M ratio is relaxed and F ratio is also kept most relaxed, more number of values present in the pro5spectrum, leading to the maximum correct classification of up to 99.5%. It is also visible from the table that, in the first quadrant, class1 is maximum and the remaining classes are also present in minimum which is considered to be the misclassification. As it is known that more and more correct

**Table 3**  
Performance of Texture Classification

M	F in %	First Quadrant				Second Quadrant				Third quadrant				Fourth quadrant			
		Class 1	2	3	4	1	Class 2	3	4	1	2	Class 3	4	1	2	3	Class 4
1%	10	79.1	19.2	0.03	1.7	1.2	79.6	5.6	13.6	1.0	1.3	88.5	9.2	0.0	2.7	15.4	81.9
	20	82.7	15.1	0.02	2.2	1.7	82.6	2.7	13.1	2.0	0.3	90.1	7.61	0.0	0.6	15.7	83.8
	25	84.6	13.0	0.01	2.4	1.3	82.7	1.3	14.7	0.0	0.4	91.3	8.38	0.0	0.0	14.0	86.0
	50	88.1	9.8	0.23	1.9	1.9	87.5	1.9	8.7	2.9	1.1	93.8	2.18	0.0	0.0	12.7	87.3
Average		83.6	14.3	0.1	2.0	1.5	83.1	2.9	12.5	1.5	0.7	90.9	6.8	0.0	0.8	14.4	84.8
5%	10	91.2	4.4	1.91	2.5	1.6	90.5	3.8	4.1	0.8	2.4	92.9	3.98	1.5	0.9	5.1	92.5
	20	93.2	6.2	0.1	0.5	1.9	92.6	4.0	1.6	0.0	0.5	93.3	6.25	1.3	0.8	5.1	92.8
	25	96.4	3.7	0.0	0.0	1.4	96.0	2.6	0.1	1.3	4.1	94.6	0.0	0.7	1.9	3.4	94.0
	50	96.8	2.5	0.0	0.7	0.5	99.5	0.1	0.0	0.2	0.8	95.1	3.99	1.0	0.0	3.7	95.3
Average		94.4	4.2	0.5	0.9	1.3	94.6	2.6	1.4	0.6	1.9	93.9	3.6	1.1	0.9	4.3	93.7

**Figure 6**  
Texture classification – Correct classification vs F ratio for the four quadrants of Figure 5



classification the misclassification will be lesser and lesser. It is also observed that the correct classification reaches maximum when the M is at 5% and F ratio is performed at 50 %.

The results are comparable with the recent publication on supervised texture classification as 98.25 % when the fabric defect classification using the machine learning techniques adapted by Yassine Ben Salem et al [19]. Hence it is observed that the proposed descriptor works well for the texture analysis problems and comparable with the other recent works. However, the attempts are made to reduce the misclassification error so as to get cent percent correct classification.

## 4. Conclusions

The presence of micro textures present in the given texture images have been successfully quantified by our proposed framework. This framework uses a set of Chebheshev orthogonal polynomials for representing the small part of the image of size 5 x 5 with the set of significant variances contributing for texture and noise. Only the contributing variances are subjected to divergence of variances test. This is varied from stringent and relaxed tolerances. The local image part is represented by a number called  $pro5num$ . The histogram of these  $pro5nums$  computed for the whole image is the  $pro5spectrum$ , which is there presentation of the entire image. Four group of interaction ef-

fects are identified and each one is experimented for a number of textured images. These representations are unique as it is evident from the graphs of spectrums. The experiments are repeated and included for classification and segmentation. Even though the grid size or image size is considered as 5 x 5, the  $pro5num$ , which are the features, ranges from 0 to 63 with 64 components, the entire texture image is represented successfully. Since the number of features are less compared to the original image size, this is computationally efficient and hence while using for other texture analysis experiments. The grid size can be further increased to 7 x 7 or 9 x 9 to perform the analysis, as the proposed set of polynomials are generalized and can be developed to any order up to n. Finally, in order to prove the efficacy of the proposed texture descriptor, a supervised texture classification has been performed with four texture classes and the correct classification up to 99.5 % could be achieved and the result is compared with recent results published in the literature. The future works involves the usage of DL model with massive Data set for performing both supervised and unsupervised texture classification experiments.

## Acknowledgement

This research was supported by a grant of the Korea Health Technology R&D Project through the Korea Health Industry Development Institute (KHIDI), funded by the Ministry of Health & Welfare, Republic of Korea (grant number : HI21C1831) and the Soonchunhyang University Research Fund.

## References

1. Bishop, D.J., Nair, U. S. A Note on Certain Methods of Testing for Homogeneity of a Set of Estimated Variances. *Biometrika*, 1939, 30, 89-99. <https://doi.org/10.2307/2983627>
2. Brodatz, P. *Texture-A Photographic Album for Artists and Designer*. Dover Publications, New York, 1966.
3. Canny, J. A Computational Approach to Edge Detection. *IEEE Transactions on PAMI*, 1986, 8(6), 679-698. <https://doi.org/10.1109/TPAMI.1986.4767851>
4. Collins, J. M., Jain, A. K. A Spatial Filtering Approach to Texture Analysis. *Pattern Recognition Letters*, 1985, 3, 195-203. [https://doi.org/10.1016/0167-8655\(85\)90053-4](https://doi.org/10.1016/0167-8655(85)90053-4)
5. Ehrlich, R. W., Foith, J. P. A View of Texture Topology and Texture Descriptors. *Computer Graphics and Image Processing*, 1978, 8, 174-202. [https://doi.org/10.1016/0146-664X\(78\)90048-5](https://doi.org/10.1016/0146-664X(78)90048-5)
6. Fisher, R. A., Yates, F. *Statistical Tables for Biological, Agricultural and Medical Research*. Oliver and Boyd, London, 1947.
7. Ganesan, L., Bhattacharyya, P. A New Statistical Approach for Micro Texture Description. *Pattern Recognition Letters*, 1995, 16(5), 471-478. [https://doi.org/10.1016/0167-8655\(95\)00123-X](https://doi.org/10.1016/0167-8655(95)00123-X)
8. Ganesan, L., Bhattacharyya, P. Edge Detection in Un-textured, Textured Images - A Common Computational

- Framework. *IEEE Transactions on SMC*, 1997, 27(5), 823-834. <https://doi.org/10.1109/3477.623235>
9. Galloway, M. M. Texture Analysis Using Gray Level Run Lengths. *Computer Graphics and Image Processing*, 1975, 4(2), 172-179. [https://doi.org/10.1016/S0146-664X\(75\)80008-6](https://doi.org/10.1016/S0146-664X(75)80008-6)
  10. Haralick, R. M. Statistical and Structural Approaches to Texture Analysis. *Proceedings of IEEE*, 1979, 67(5), 786-804. <https://doi.org/10.1109/PROC.1979.11328>
  11. He, D. C., Wang, L. Texture Unit, Texture Spectrum for Texture Analysis. *IEEE Transactions on Geo Science and Remote Sensing*, 1990, 28(4), 509-512. <https://doi.org/10.1109/TGRS.1990.572934>
  12. Jain, A. K., Ferrokhnia, F. Unsupervised Texture Segmentation Using Gabor Filters. *Pattern Recognition*, 1991, 24(12), 1167-1186. [https://doi.org/10.1016/0031-3203\(91\)90143-S](https://doi.org/10.1016/0031-3203(91)90143-S)
  13. Tuceryan, T., Jain, A. K. *Texture Analysis in Handbook of PR and CV*. World Scientific Publishing Company USA, 1988.
  14. Weszka, J. S., Dyer, C. R., Rosenfeld, A. A Comparative Study of Texture Measures for Terrain Classification. *IEEE Transactions on SMC*, 1976, 6, 269-285. <https://doi.org/10.1109/TSMC.1976.5408777>
  15. Qinghe, Z., Yang, M., Yang, J., Zhang, Q., Zhang, X. Improvement of Generalization Ability of Deep CNN via Implicit Regularization in Two-stage Training Process. *IEEE Access*, 2018, 6, 15844-15869. <https://doi.org/10.1109/ACCESS.2018.2810849>
  16. Qinghe, Z., Tian, X., Yang, M., Wu, Y., Su, H. PAC-Bayesian Framework Based Drop-path Method for 2D Discriminative Convolutional Network Pruning. *Multidimensional Systems and Signal Processing*, 2020, 31(3), 793-827. <https://doi.org/10.1007/s11045-019-00686-z>
  17. Zheng, Q., Yang, M., Tian, X., Jiang, N., Wang, D. A Full Stage Data Augmentation Method in Deep Convolutional Neural Network for Natural Image Classification. *Discrete Dynamics in Nature and Society*, 2020, 1-11. DOI: 10.1155/2020/4706576. <https://doi.org/10.1155/2020/4706576>
  18. Zheng, Q., Zhao, P., Li, Y., Wang, H., Yang, Y. Spectrum Interference-based Two-level Data Augmentation Method in Deep Learning for Automatic Modulation Classification. *Neural Computing & Applications*, 2020. <https://doi.org/10.1007/s00521-020-05514-1>
  19. Yassine, B. S., Abdelkrim, M. Texture Classification of Fabric Defects Using Machine Learning. *International Journal of Electrical and Computer Engineering*, 2020, 10(4), 4390-4399. <https://doi.org/10.11591/ijece.v10i4.pp4390-4399>
  20. [vismod.media.mit.edu/vismod/imagery/VisionTexture](http://vismod.media.mit.edu/vismod/imagery/VisionTexture)

